PROCEEDINGS, Twelfth Workshop on Geothermal Reservoir Engineering
Stanford University, Stanford, California, January 20-22, 1987
SGP-TR-109

Analysis of Thermally Induced Permeability Enhancement in Geothermal Injection Wells

S. M. Benson and J.S. Daggett

Earth Sciences Division
Lawrence Berkeley Laboratory
Berkeley, California 94720

E. Iglesias, V. Arellano, and J. Ortiz-Ramirez

Instituto De Investigaciones Electricas
Departamento De Geotermia
Cuernavaca, Morelos, Mexico

ABSTRACT

Reinjection of spent geothermal brine is a common means of disposing of geothermal effluents and maintaining reservoir pressures. Contrary to the predictions of two-fluid models (two-viscosity) of nonisothermal injection, an increase of injectivity, with continued injection, is often observed. Injectivity enhancement and thermally-affected pressure transients are particularly apparent in short-term injection tests at the Los Azufres Geothermal Field, Mexico. During an injection test, it is not uncommon to observe that after an initial pressure increase, the pressure decreases with time. As this typically occurs far below the pressure at which hydraulic fracturing is expected, some other mechanism for increasing the near-bore permeability must explain the observed behavior. This paper focuses on calculating the magnitude of the near-bore permeability changes observed in several nonisothermal injection tests conducted at the Los Azufres Geothermal Field. In order to evaluate the pressure transient data and calculate the magnitude of the thermally induced permeability changes, a new analytic solution for calculating pressure transients with time-varying sandface flowrates and temperatures has been developed. The effects of temperature-dependent fluid and rock properties, as well as a moving thermal front, are explicitly included in the calculations. Based on this new solution, a technique is developed for calculating the reservoir permeability, skin factor of the well, and near-bore permeability increases. The results of these calculations indicate that the permeability increases by a factor of 5 in the near-bore region during the 2 to 3 hour injection tests. A good correlation between the permeability increase and the sandface injection temperature indicates that the permeability increase is caused by cooling the formation.

INTRODUCTION

Injecting cold water is a common technique for estimating the permeability, productivity, and injectivity of geothermal wells. In addition to providing a measure of these parameters, there is some evidence that this practice stimulates the well (Bodvarsson et al., 1984). This is contrary to the predictions of physical and mathematical models that consider only the temperature dependent fluid properties (Benson, 1984; Benson and Bodvarsson, 1986).

This intriguing phenomena is particularly apparent in geothermal wells in the Los Azufres Geothermal Field in Mexico, where a large set of pressure transient data exhibit unusual characteristics. As shown by pressure buildup curves for three wells in Figure 1, it is not uncommon to observe that after an initial period during which the pressure increases as expected, the pressure stabilizes and then begins to drop, even though injection continues at a steady rate. This unusual behavior is attributed to progressive increases in the near-bore permeability. Several physical mechanisms can increase the near-bore permeability, including; hydraulic fracturing, pushing drilling mud and formation fines away from the well-bore and into the formation, thermal contraction and thermal stress cracking of the rock, and dissolution of fracture filling minerals. As these tests were conducted well below the fracture gradient, hydraulic fracturing has been eliminated as a possible cause for the permeability increase, leaving one or more of the other mechanisms to account for the observed behavior.

The goal of this investigation is two-fold. First we attempt to quantify the magnitude of the permeability increase needed to explain the observed pressure behavior. Next, we investigate correlations between temperature and the permeability increase in an effort to provide insight into the physical mechanism governing this occurrence.

BACKGROUND

It is worthwhile to spend a moment reviewing the physical processes that occur as cold water is injected into a hot geothermal reservoir. First, injection causes the pressure to increase due to the formation's resistance to flow. For horizontal flow in a liquid saturated rock, the pressure buildup is governed by Equation 1

$$\nabla\cdot(\frac{k\,\rho}{\mu}\nabla p\,) = \frac{\partial(\rho\phi)}{\partial p}\frac{\partial p}{\partial t} \qquad (1)$$

where k is the formation permeability, ρ is the fluid density, μ is the fluid viscosity, p is the fluid

pressure, and ϕ is the porosity of the formation. Second, as fluid is injected into the well, an interface (called the hydrodynamic front) between the undisturbed reservoir fluids and the injected fluid moves away from the injection well. The thermal front (defined as the surface where the temperature is midway between the temperature of the reservoir and injected fluids) lags some distance behind the hydrodynamic front due to a transfer of heat from the reservoir rock to the injected fluid. The distance to these fronts (r_f) and the rate at which they move away from the injection well depend on the relevant mass and energy conservation equations and the geometry of the system. In the region behind the fronts, the composition, temperature, compressibility (c_f) and density of the fluid may be different than the in-situ fluid. In addition, if the permeability, porosity, and pore-volume compressibility (c_{pv}) are temperature, stress, or composition sensitive, they too may vary in the region behind the front.

The wellbore also influences the pressure changes caused by injection. In deep geothermal systems the typically large wellbores create significant wellbore storage effects, resulting in a long time period before the surface and sandface injection rates are equal. Second, the wellbore acts like a large heat exchanger, transferring heat from the formation to the injected fluid before in is injected into the open interval of the well. This results in a time-varying sand-face injection temperature. At moderate injection rates it may take several hours for the sandface injection temperature to stabilize.

MATHEMATICAL MODEL

Having reviewed the range of physical processes controlling the pressure buildup during injection, we are ready to choose a mathematical model for interpreting the data. There is a small but relevant collection of papers devoted to the interpretation of injection tests. However, all of these models consider only that the properties of the injected fluid are different from the properties of the in situ fluid. Nevertheless, they provide valuable insight into the pressure transient behavior. Consequently, they are reviewed briefly below.

A closed form analytical solution for Equation 1 has been derived for the special case where the volumetric injection rate (Q) is constant and

$$r_f(t) = \left[\frac{bQt}{\pi h}\right]^{1/2} \tag{2}$$

where b is a constant that depends on the relevant mass and/or energy balances and h is the thickness of the formation, provided that the properties of the fluid and formation behind the front are uniform and constant (Ramey, 1970). For nonisothermal injection

$$b = \frac{\rho_w C_w}{\rho_a C_a} \tag{3}$$

where C_w and C_a are the heat capacity of the injected water and reservoir, and ρ_w and ρ_a are the density of water and the reservoir, respectively. Although, this solution can be extended to consider the effects of increasing near-bore permeability, several other important factors, such as varying

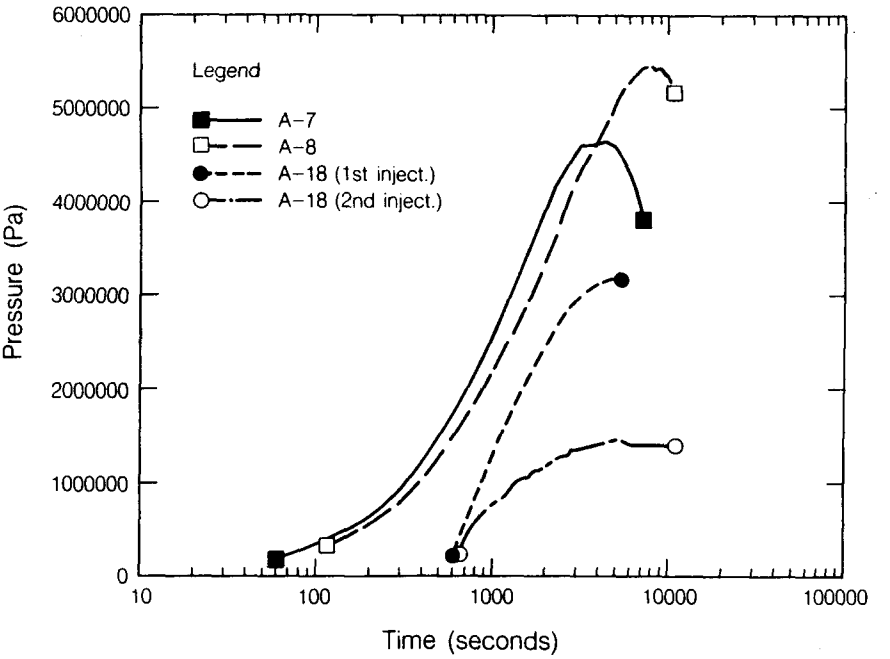

Figure 1. Pressure transient data from four injection tests at the Los Azufres Geothermal Field.

flowrates and time-dependent sandface injection temperatures can not be included.

Numerical solutions of Equation 1 have also provided insightful descriptions of pressure transient behavior during nonisothermal and multicomponent injection. An extensive study of the influence of temperature dependent fluid viscosity and density on the pressure transient behavior, resulted in developing injection test analysis methods and front tracking techniques under certain idealized conditions (Benson, 1984; Benson and Bodvarsson, 1986). Additional studies by Cox and Bodvarsson (1985) investigate pressure transients during nonisothermal injection into a horizontally and vertically fractured formation.

A review of the literature shows that although Equation 1 has been solved for some special cases where the properties of the injected fluid differ from the injected system, in general, we are still restricted to a two-fluid model, where the properties are uniform within each of the two regions. Furthermore, using currently available solutions, we are restricted to studying systems where the movement of the front is described by Equation 2. Other restrictive factors include requiring that the rock properties remain constant, that the injection rate remains constant or is a series of step rates, and the properties of the fluid remain constant during injection. As discussed above in actual field tests, many of these conditions are violated, rendering the currently available solutions inadequate.

New Solution

To circumvent the restrictive assumptions required to develop a closed form analytic solution to Equation 1, an alternative approximate solution of the form

$$\Delta p\,(r_w\,,t\,) = \Delta p_{ss}\,(r_w\,,t\,)+\Delta p_t\,(r_f\,,t\,) \qquad (4)$$

is proposed, where $\Delta p\,(r_w\,,t\,)$ is the pressure change at the injection well, $\Delta p_{ss}\,(r_w\,,t\,)$ is the steady-state pressure change across the invaded region at time t, and $\Delta p_t\,(r_f\,,t\,)$ is the transient pressure response in the uninvaded formation. The mathematical advantages of this form of the solution are twofold. First, all of the non-linear terms associated with the region behind the front in Equation 1 are incorporated into the first term of Equation 4, which for a slightly-compressible single component fluid flowing through a radially symmetric system is calculated by

$$\Delta p_{ss}\,(t\,) = \frac{q}{2\pi h}\int_{r_w}^{r_f\,(t\,)} \frac{\mu(r\,,t\,)}{k\,(r\,,t\,)\,\rho(r\,,t\,)}\,\frac{dr}{r} \qquad (5)$$

where q is the mass injection rate and the other terms are defined as before. Second, the term $\Delta p_t\,(r_f\,,t\,)$ can easily be evaluated from well established solutions such as the exponential integral solution, convolution of the instantaneous line source solution for variable flow rates, or any one of a number of relevant solutions that satisfy the desired outer boundary conditions.

With the utility of Equation 4 established, it becomes important to determine the range of conditions under which it is valid. The condition that pseudo-steady flow conditions exist within the invaded region is implicit in Equation 4. This condition is approximately satisfied for

$$t > \frac{25\,r_f^{\,2}}{\eta_1} \qquad (6)$$

where η_1 is the diffusivity $(k\,/\phi\mu c_t\,)$ of the inner region. Evaluation of Equation 6 for a wide range of formation parameters and fluid properties shows that Equation 4 is valid within several seconds after injection begins if r_f (at $t=0$)$=r_w$.

Verification

As an example how Equation 4 is applied in a typical situation, it will be compared to the closed form analytical solution for nonisothermal injection of a fluid at a temperature of T_i (with properties μ_i and ρ_i) into a uniform, areally infinite, porous media with constant rock properties, that is originally at temperature of T_r (with properties μ_r and ρ_r). In this case, the radial distance to the thermal front is given by

$$r_f\,(t\,)=\left[\frac{\rho_w\,C_w\,Qt}{\rho_a\,C_a\,\pi h}+r_w^{\,2}\right]^{1/2} \qquad (7)$$

For uniform fluid properties, and constant rock properties behind the front, the first term in Equation 4 (evaluated by integrating Equation 5) is given by

$$\Delta p_{ss}\,(r_w\,,t\,) = \frac{q\,\mu_i}{2\pi\rho_i\,kh}\ln\left(\frac{r_f}{r_w}\right) \qquad (8)$$

The second term in Equation 4 is evaluated with the exponential integral solution (Ei) and is given by

$$\Delta p_t\,(r_f\,,t\,)=\frac{q\,\mu_r}{4\pi\rho_r\,kh}Ei\left(\frac{r_f^{\,2}}{4\eta_r\,t}\right) \qquad (9)$$

Adding Equations 8 and 9 together, and recognizing that the asymptotic expression for the exponential integral (Ei) is appropriate in this case, we see

$$\Delta p\,(r_w\,,t\,) = \frac{q\,\mu_r}{4\pi\rho_r\,kh}\left[\frac{\mu_r\,\rho_i}{\mu_i\,\rho_r}\ln\left(\frac{r_f}{r_w}\right)^2+\ln t\right.$$

$$\left.+\ln\left(\frac{\eta_r}{r_f^{\,2}}\right)+0.80907\right] \qquad (10)$$

The closed form analytic solution for the same problem is given by

$$\Delta p\,(r_w, t) = \frac{q\,\mu_i}{4\pi\rho_i\,kh}\left[Ei\left(\frac{r_w{}^2}{4\eta_i\,t}\right) - Ei\left(\frac{r_f{}^2}{4\eta_i\,t}\right)\right] + \frac{q\,\mu_r}{4\pi\rho_r\,kh}\,e^{\frac{-r_f{}^2}{4\eta_i}\left(1-\frac{\eta_i}{\eta_r}\right)}\,Ei\left(\frac{r_f{}^2}{4\eta_r\,t}\right) \qquad (11)$$

For a slightly compressible fluid, the exponential expression in the second term of Equation 11 is within 1% of unity within several seconds after injection begins. Also, as in the above case, the asymptotic approximation for the Ei function is appropriate. Under these conditions, the sum of the two terms inside the brackets is equal to $\ln(r_f/r_w)^2$ and Equation 11 can be rearranged to produce a result that is identical to Equation 10.

In addition to comparing Equation 4 to the closed form analytical solution for a two-fluid system, mathematical solutions generated with Equation 4 have been verified by comparison to numerically simulated pressure transients during nonisothermal injection in geothermal reservoirs. Results have been compared for variable and steady injection rates in porous systems, as well as for steady injection rates in horizontally and vertically fractured geothermal reservoirs. In all cases, agreement between the two methods is excellent, as long as Equation 6 is satisfied.

ANALYSIS METHOD

Before analyzing the pressure transient data from any injection test, it is necessary to carefully assess all of the salient features of the test data. Once these have been established, a mathematical solution tailored to the problem at hand, can be developed by applying Equations 4 and 5.

The Los Azufres geothermal system occurs in fractured volcanic deposits, at a depth of 1000 to 2000 m. Reservoir temperatures range from 220 to 280 ° C in the wells from which injection test data are available. Geothermal fluids are produced from fractured horizons within andesitic rocks. The injection tests consisted of injecting 20 ° C water into the formation at a constant wellhead injection rate for 2 to 3 hours. During injection, the formation pressure was measured with an Amerada pressure gauge positioned adjacent to the production zone in the well.

Log(pressure) vs. log(time) graphs (not shown here) of the pressure buildup data shown in Figure 1 indicate that wellbore storage effects persist throughout the entire 2 to 3 hour test. This is illustrated in Figure 2, which shows the sandface injection rate as a function of time for well A-7. For the first half of the test, the sandface injection rate gradually increases to the surface injection rate. During the latter half of the test, the sandface injection rate is greater than the surface

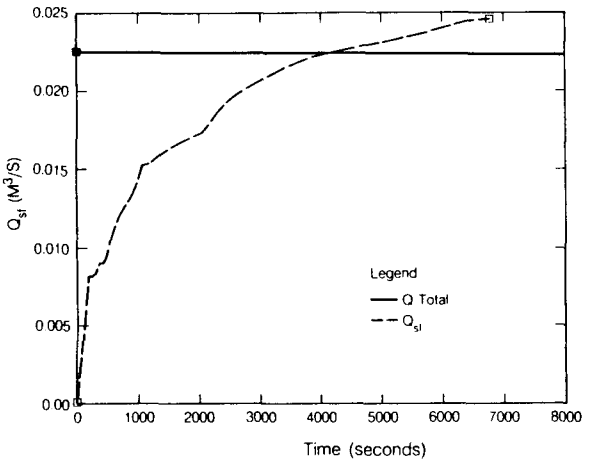

Figure 2. Sandface flowrate during the well A-7 injection test.

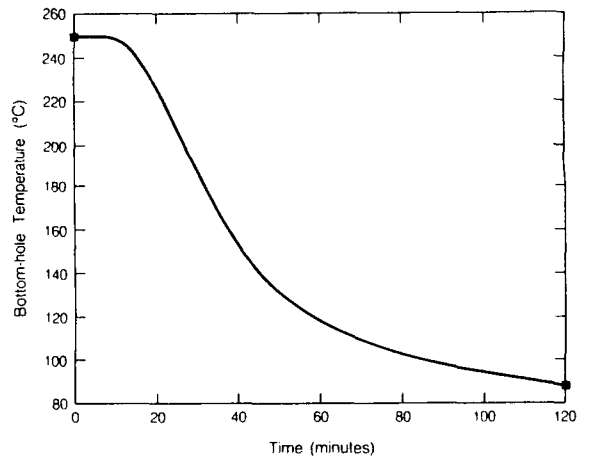

Figure 3. Simulated sandface temperature during the well A-7 injection test.

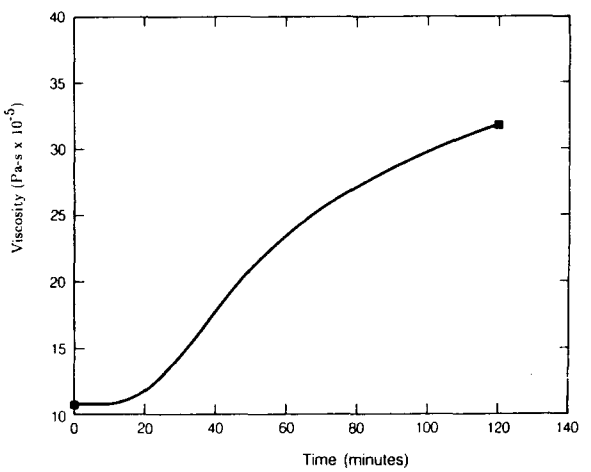

Figure 4. Sandface fluid viscosity during the well A-7 injection test.

injection rate because the pressure (waterlevel) is dropping in the wellbore.

Another factor that must be considered is that although the temperature of the injected water is constant at the wellhead, it is not constant at the formation face. As shown by the simulated sandface injection temperature in Figure 3, the sandface temperature decreases throughout the test. By the end of the test, the temperature is still nearly 70 °C above the surface temperature. The time-varying injection temperature causes the fluid viscosity (see Figure 4) and density to vary throughout the test. This creates a non-uniform distribution of the fluid properties in the region behind the front.

In light of these complications, one might deduce that there is little chance of obtaining any valuable information from this test data. However, by making a few assumptions, which will be discussed below, and applying a solution generated from Equation 4, we are able to determine the formation permeability, and estimate the magnitude of the thermally-induced permeability enhancement that causes the unusual pressure transient response.

To develop a mathematical solution for calculating the pressure buildup, we must first describe how the front moves with time. For the purposes of this analysis, the distance to the front, based on an energy balance between the heat lost from the rock and that gained by the injected fluid, is assumed to be given by

$$r_f^{\,2} = \frac{\rho_w C_w}{\rho_a C_a} \frac{1}{\pi h} \int_0^t Q(t)\,dt \qquad (12)$$

where C_w and C_a are the heat capacities of water and the formation, respectively and the other terms are as defined previously. Note that this formulation assumes that there is no heat transfer between the low permeability rock formation and the permeable layers into which fluid is injected. Although this is not generally true for fractured reservoirs, this assumption is justified in light of the short duration of the tests and that fluid is injected into a "fracture zone" that is much thicker than the apertures of individual fractures. If the fluid is injected into very thin strata, separated by much thicker strata, the effects of heat conduction to the surrounding strata must be considered (Bodvarsson and Tsang, 1982).

It is also necessary to describe how the fluid properties vary behind the front. For this study we assume that the fluid viscosity and density, as well as, the formation permeability vary linearly in the region behind the front

$$\mu_i(r,t) = \mu_i(r_w,t) + \frac{\mu_r - \mu_i(r_w,t)}{r_f - r_w}(r - r_w)$$

$$\rho_i(r,t) = \rho_i(r_w,t) + \frac{\rho_r - \rho_i(r_w,t)}{r_f - r_w}(r - r_w)$$

$$k_i(r,t) = k_i(r_w,t) + \frac{k_r - k_i(r_w,t)}{r_f - r_w}(r - r_w) \qquad (13a, b, c)$$

We could equally well choose some other functional form for describing how these properties vary behind the front. These ones are chosen for simplicity and lack of data suggesting that some other form is more appropriate. By substituting Equations 13a to 13c into Equation 5, we can calculate the steady-state pressure buildup in the region behind the front from

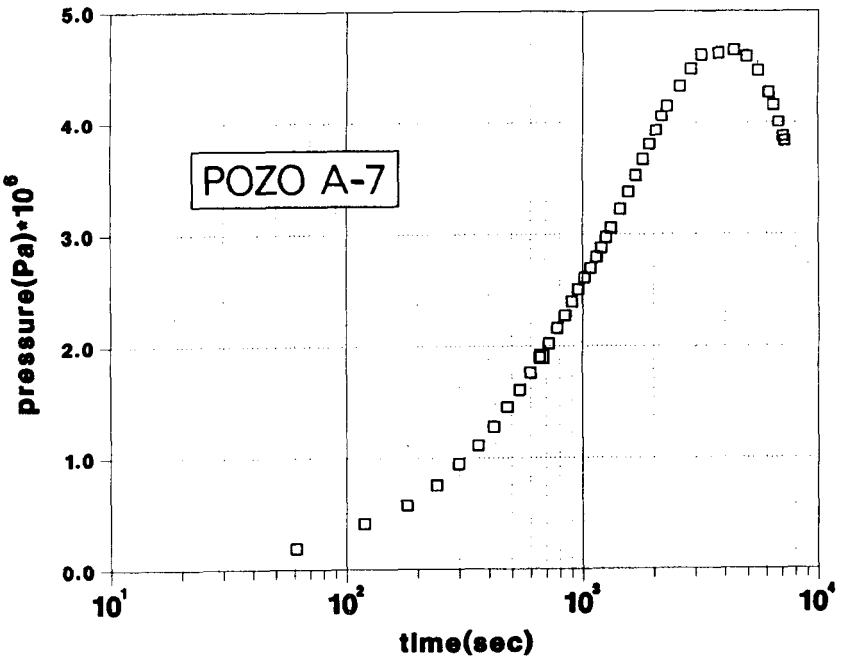

Figure 5. Pressure transient data from the well A-7 injection test.

$$\Delta p_{ss}(t) = \frac{q(t)}{2\pi h}\left[\frac{\mu_i(r_w,t)}{k_i(r_w,t)\rho_i(r_w,t)}\ln\frac{r_f}{r_w} + \left(\frac{\mu_r}{k_r\rho_r} - \frac{\mu_i(r_w,t)}{k_i(r_w,t)\rho_i(r_w,t)}\right)\left[1 - \frac{r_w}{r_f - r_w}\ln\frac{r_f}{r_w}\right]\right] \quad (14)$$

To develop a full solution to Equation 4 we also need an expression for calculating the transient pressure response in the uninvaded region of the reservoir. For this study we assume that the reservoir is approximately described as a uniform porous media, of infinite areal extent, and bounded above and below by impermeable strata. For this type of system, the second term of Equation 4 can be evaluated easily if the time-varying flow rate is represented by a sequence of straight line segments, each of the proper duration and slope (McEdwards and Benson, 1981). The full solution to Equation 4 is calculated by adding Equation 14 to the pressure transient response in the outer region. A computer program that performs the necessary calculations has been written.

Three primary variables must be determined to analyze the pressure buildup tests. These include the permeability-thickness product (kh) of the fracture zones, the mechanical skin factor of the well (s_m), and the magnitude of the near-bore permeability enhancement. A two-stage analysis method is required for evaluating all of these parameters. First, kh and s_m are calculated from the early part of the pressure buildup data when the nonisothermal effects are small. As shown by Figures 3 and 4, this period lasts approximately for 15 minutes. Although this early time data is strongly influenced by wellbore storage, a history-match of the data can be used to calculate kh and s_m by using the variable flowrate algorithm described above (McEdwards and Benson, 1981; and Bodvarsson et al., 1984). Once these two parameters are established, the remainder of the test data are used to calculate the magnitude of the near-bore permeability changes that occur as the progressively colder water is injected into the formation.

The procedure for doing this is as follows. First, the pressure buildup ($\Delta p_i(r_w,t)$) for an isothermal injection test (at the formation temperature) is calculated using the formation parameters obtained from the initial step of the analysis. Next, the difference between $\Delta p_i(r_w,t)$ and the actual pressure response is used to calculate the near-bore permeability change from the following expression

$$\frac{k_r}{k_i(r_w,t)} = \frac{\mu_r\,\rho_i(r_w,t)}{\mu_i(r_w,t)\rho_r}\left\{\frac{\frac{2\pi k_r\rho_r h}{q\mu_r}\left(\Delta p(r_w,t) - \Delta p_i(r_w,t)\right) - s_{ma} + s_m}{\left[\left(1+\frac{r_w}{r_f - r_w}\right)\ln\frac{r_r}{r_w} - 1\right]} + 1\right\} \quad (15)$$

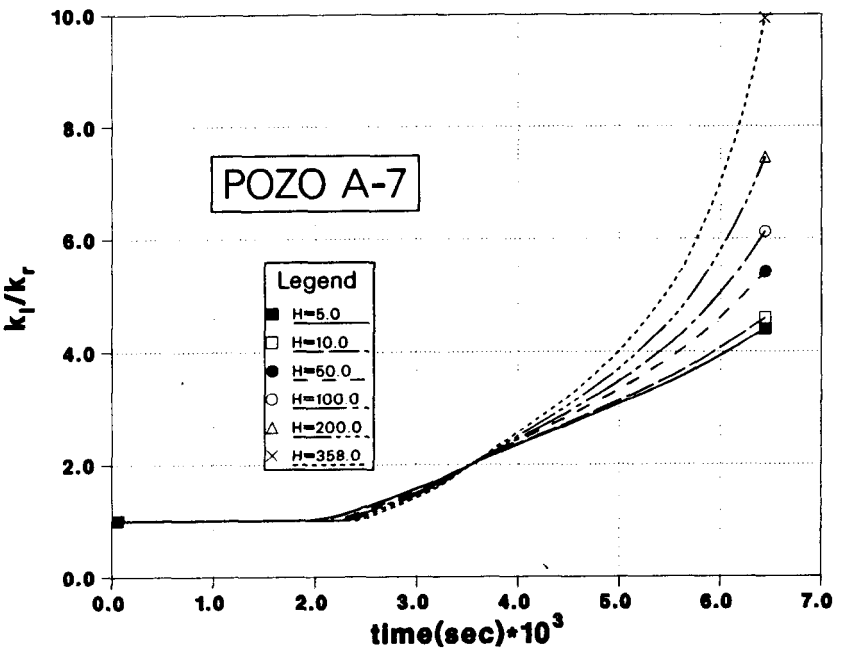

Figure 6. Calculated permeability enhancement during the well A-7 injection test for a range of assumed values for the formation thickness.

where s_{ma} is the apparent-mechanical skin factor of the well. For $s_m > 0$

$$s_{ma} = \frac{\mu_i(r_w, t)\rho_r}{\mu_r \rho_i(r_w, t)} s_m \qquad (16a)$$

and for $s_m << 0$

$$s_{ma} = s_m \qquad (16b)$$

(Benson, 1984).

Each of the four injections tests shown in Figure 1 have been analyzed using the above procedure. The analysis of the data from well A-7 is reviewed in detail.

Well A-7 Analysis

The injection test data for well A-7 are shown in Figure 5. The sandface injection rate, temperature, and fluid viscosity are shown in Figures 2 through 4, respectively. For the first 15 minutes of the test, the bottomhole temperature remained at approximately 250 °C. A history match of this data yields a kh of $3x\ 10^{-13}$ m^3 and a mechanical skin factor of -2. After the first fifteen minutes, the temperature sensitive rock and fluid properties begin to influence the data. Using the procedure outlined above, the ratio of the undisturbed formation permeability to the permeability of the invaded region immediately adjacent to the wellbore is calculated for the rest of the test period. The results of these calculations are shown in Figure 6, where the ratio of $k_i(r_w, t)/k_r$ is plotted as a function of time from the beginning of the injection test. The ratio is plotted for a range of values for the formation thickness because we do not have an accurate measure of the thickness of the zone(s) into which the fluid is injected. The figure shows that the permeability of the near-bore region must increase by a factor ranging from 4 to 10 over the 2 hour test, depending on the actual thickness of the formation. Figure 6 also demonstrates that if the formation thickness is less than 50 m, the results of the calculation are relatively insensitive to the actual value of the formation thickness. The fractured nature of the producing formation and the occurrence of discrete loss-of-circulation zones encountered while drilling these wells suggests that the actual thickness is in the range of 5 to 10 m. Thus, the permeability appears to increase by a factor of 5 over the test period.

Once the formation parameters and the magnitude of the near-bore permeability increases are determined, these calculations can be double-checked by comparing the measured pressure response to the calculated response. Figure 7 shows the comparison for well A-7.

Another source of uncertainty in this analysis is the actual distribution of the fluid and rock properties within the invaded region. As mentioned above, we assume that these vary linearly. To test the restraints imposed on the analysis by this assumption, we repeated these calculations for the case where the fluid and rock properties are constant throughout the invaded region. The results of these calculations are shown in Figure 8, where $k_i(r_w, t)/k_r$ is calculated for formation thicknesses of 5 and 10 m. These calculations show the results are relatively insensitive to the presumed distribution of the various parameters. This is explained in light of the dominating influence of the very near-well region on the pressure response, which is nearly the same, regardless of how the properties are distributed farther away from the well.

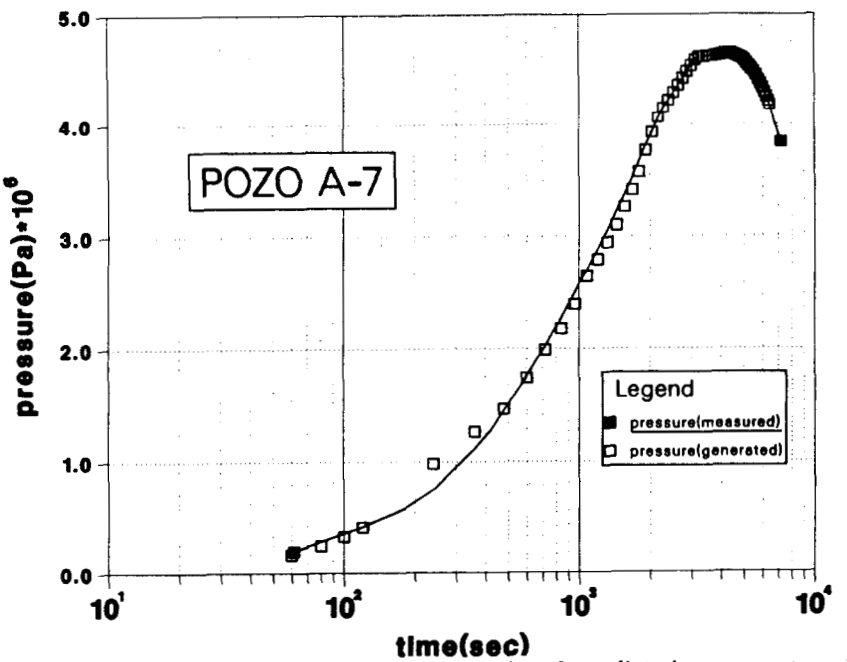

Figure 7. Match between the measured and predicted pressure transient response during the well A-7 injection test.

RESULTS

The magnitude of the near-bore permeability enhancement in each of the 3 test wells (A-7, A-8, and A-18) is plotted as a function of the sandface injection temperature in Figure 9. For the well A-18, the permeability increase during a second injection test is also plotted. The calculated permeability increases for wells A-7, A-8, and the first test of A-18 are remarkably similar, suggesting that the correlation between the sandface injection temperature and the permeability increase is attributable to the thermal characteristics of the rock mass. On the other hand, the larger increase in the permeability calculated from the second test in well A-18 suggests that the effects of heating and cooling are cumulative. This suggests that stress changes occurring during injection also influence the permeability increase. The readjustments of the contact points between the opposing walls of the frac-

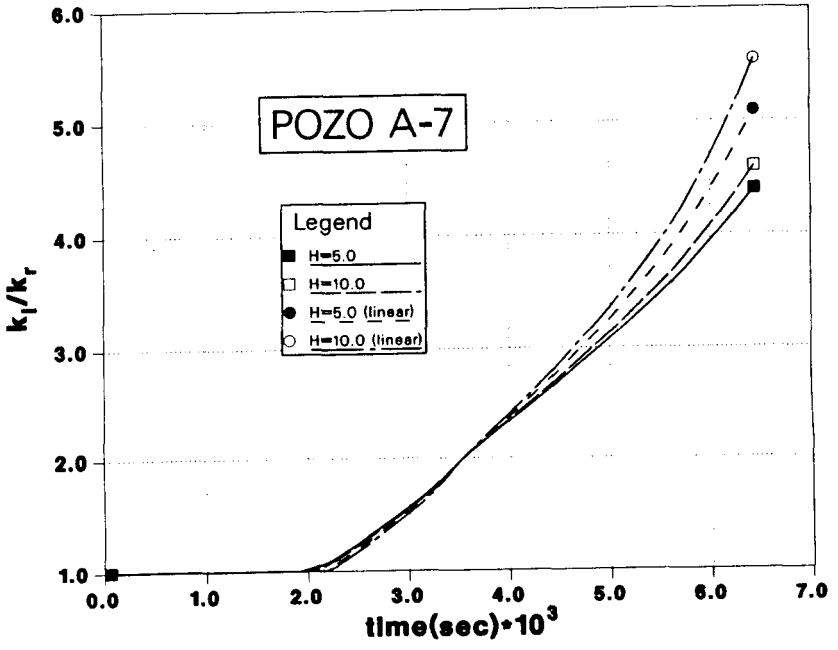

Figure 8. Comparison between the calculated permeability enhancement for a linear and a uniform distribution of fluid and rock properties in the region behind the front.

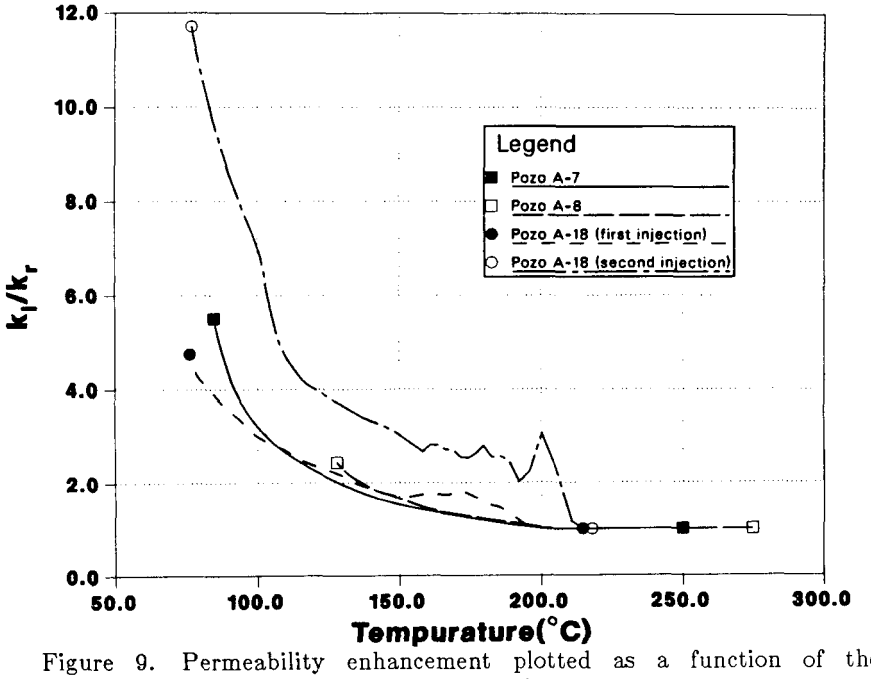

Figure 9. Permeability enhancement plotted as a function of the sandface injection temperature for four injection tests.

tures that take place in response to pore pressure increases and thermal contraction of the rock may result in permanent increases in the near-bore permeability as the result of injecting cold water into a geothermal formation.

There are several possible explanations for the observed temperature versus permeability relationship, including; thermal stress cracking, dissolution of the formation, and thermal contraction of the rock matrix. In the absence of additional information, we can not decide which amongst these possibilities is the correct one, nor if a single mechanism is responsible for the observed behavior. Recent laboratory studies of thermal stress cracking indicate that both intragranular and grain-boundary stress cracks can develop in the thermal regime in which these tests are conducted (Fredrich and Wong, 1986). Analysis of field experiments at the hot-dry-rock site at Fenton Hill indicate that "reservoir growth" can be at least partially attributed to thermally induced stress cracks (Tester et al., 1986). It is likely that a similar mechanism is responsible for the permeability enhancement observed in the data described here.

The analysis presented here is just the beginning of a series of studies that must be conducted if we are to improve our understanding of the physical phenomena that accompany reinjection into geothermal reservoirs. To date, we do not have an adequate physical understanding of the physical mechanisms causing the unusual pressure transients responses nor the observations that well injectivity is often better than anticipated. The possibility that the observed permeability increases may be permanent or semi-permanent is also intriguing. If so, cold water injection may come to be considered as a bona fide stimulation treatment for geothermal wells.

CONCLUSION

Analysis of injection test data from three wells at the Los Azufres geothermal field in Mexico indicate that the permeability of the near-bore region increases during cold water injection. Careful examination of the data reveal that an accurate analysis of the data is impossible if wellbore storage effects and thermal transients in the wellbore are not accounted for in the analysis. By using a new analysis method that is outlined in this paper, the magnitude of the permeability increase that is required to match the observed pressure transient data is calculated for each of the wells. These analyses indicate that the permeability increases by approximately a factor of 5 in the near-bore region during the 2 to 3 hour period when cold water is injected into the formation. A good correlation between the permeability increase and the sandface injection temperature indicates that the permeability increase is caused by cooling the formation. Thermal contraction and thermal stress cracking of the formation are the most probable cause of the near-bore permeability increase.

ACKNOWLEDGEMENTS

This work is supported through the U.S. Department of Energy Contract No. DE-AC03-76SF00098 by the Assistant Secretary for Conservation and Renewable Energy, Office of Renewable Technology, Division of Geothermal Technology.

REFERENCES

Benson, S.M., 1984. Analysis of Injection Tests in Liquid Dominated Geothermal Reservoirs. M.S. Thesis, University of California, Berkeley, California, Lawrence Berkeley Laboratory Report, LBL-17953, Berkeley, California.

Benson, S.M. and Bodvarsson, G.S., 1986. Non-isothermal Effects During Injection and Falloff Tests, Society of Petroleum Engineers Formation Evaluation, February, 1986, pp. 53-63.

Bodvarsson, G.S., Benson, S.M., Sigurdsson, O., Stefansson, V., and Eliasson, E.T., 1984. The Krafla Geothermal Field, Iceland: 1. Analysis of Well Test Data, Water Resources Research, Vol 20, No. 11, pp. 1515-1530.

Bodvarsson, G.S. and Tsang, C.F., 1982. Injection and Thermal Breakthrough in Fractured Geothermal Reservoirs, Journal of Geophysical Research, Vol. 84, No. B2, pp. 1031-1048.

Cox, B.L., and Bodvarsson, G.S., 1985. Nonisothermal Injection Tests in Fractured Reservoirs, Proceedings, Tenth Workshop on Geothermal Reservoir Engineering, Stanford University, Stanford, California, pp. 151-162.

Fredrich, J.T., and Wong, T., 1986. Micromechanics of Thermally Induced Cracking in Three Crustal Rock, Journal of Geophysical Research, V. 91, No. B12, pp. 12743-12764.

McEdwards, D.G. and Benson, S.M., 1981. User's Manual for ANALYZE-- A Variable-Rate, Multiple Well, Least Squares Matching Routine for Well Test Analysis, Lawrence Berkeley Laboratory Report, LBL-10907, Berkeley, California.

Ramey, H.J. Jr., 1970. Approximate Solutions for Unsteady Liquid Flow in a Composite Reservoir, Journal of Canadian Petroleum Technology, March, 1970, pp. 32-37.

Tester, J.M., Murphy, H.D., Potter, R.M., and Robinson, B.A., 1986. Fractured Geothermal Reservoir Growth Induced By Heat Extraction. Society of Petroleum Engineers Paper SPE-15124. Presented at the 56th California Regional Meeting of the Society of Petroleum Engineers, Oakland, California, April 2-4, 1986.